Composites Science and Technology **34** (1989) 267–283

Failure Mechanisms in Glassy-Metal-Reinforced Epoxy Composites

It-Meng Low

Department of Chemical and Materials Engineering, University of Auckland, Private Bag, Auckland, New Zealand

Gary Hewitt, Yiu-Wing Mai*

Department of Mechanical Engineering, University of Sydney, Sydney NSW 2006, Australia

&

Cathy Foley

Division of Applied Physics, CSIRO, Lindfield NSW 2070, Australia

(Received 25 May 1988; revised version received 22 July 1988; accepted 6 August 1988)

ABSTRACT

Epoxy composites containing both rubbery particles and short or continuous glassy metal ribbons are investigated. Considerable improvement in the fracture toughness, K_{Ic}, has been obtained, particularly in composites containing aligned short ribbons where K_{Ic} values greater than 4 $MPa\sqrt{m}$ may be achieved. As the volume fraction of the ribbon is increased, so is the fracture toughness. The micromechanisms of toughening and failure processes have also been identified and discussed in the light of the microstructures.

* To whom all correspondence should be addressed.

1 INTRODUCTION

For a material to qualify as a successful high-performance engineering material, it must satisfy two major requirements, namely (i) good mechanical properties and (ii) sufficient fracture toughness. Pure epoxy resins have most of the former attributes and excellent corrosion resistance, but they lack the latter. Consequently, various techniques have been developed to improve the fracture resistance of epoxy resins without seriously affecting their mechanical properties. Essentially, these techniques involve introduction into the resin of dispersed phases which may be rigid particulate material or fibres,[1-3] rubbery particles[4-6] or both.[7-9] Significant improvement in fracture toughness has been recorded in such modified epoxies, particularly those containing both rubbery and short fibres,[9] which may serve as potential high-performance engineering adhesives and/or matrix materials for fibre composites.

Recent developments in the production of glassy metals have indicated that these materials may prove attractive as reinforcements for epoxy resins. These new materials have already been used as corrosion-resistant reinforcements for mortar[10] and as reinforcing fillers for polyester[11] and epoxy resins.[12-15] Depending on the alloy compositions used, the glassy metal can have a variety of technologically useful properties such as high strength, high hardness, soft magnetic properties and good corrosion resistance[16] which may be readily imparted to the composites. A significant improvement in the fracture energy of mortar was reported by Argon *et al.*,[10] where the introduction of 0·01 volume fraction of Metglas ribbons gave a 2300-fold increase in the specific fracture work. In glassy metal–epoxy resin composites even a very small (0·002) volume fraction of ribbons can double the fracture toughness.[15] Chand *et al.*[11] and Strife and Prewo[17] observed an increase in tensile strength and elastic modulus in their glassy metal modified plastics.

In this paper, we present some results on the microstructure–property relationship in a rubber toughened epoxy resin modified with various amounts of short and continuous glassy metal ribbons. The fracture properties of these modified epoxies are discussed in relation to their microstructures. Failure and toughening mechanisms in these materials are also identified with the aid of scanning electron microscopy. This work differs from the previous work of Friedrich and co-workers on metallic glass/epoxy resin composites[14,15] on three points. Firstly, we have used a rubber toughened epoxy resin matrix; secondly, we have studied the effect of volume fraction of ribbons over a wider range that is covered in Refs 14 and 15; and thirdly, both continuous and short ribbons are used in this study.

2 EXPERIMENTAL PROCEDURE

The epoxy resin used was Ciba Geigy GY250 (Australia Pty Ltd, Sydney), a diglycidyl ether of bisphenol A (DGEBA). The curing agent was piperidine and the rubber used was a carboxyl-terminated, random copolymer of butadiene acrylonitrile, CTBN (1300 × 13), obtained from BF Goodrich (Australia Pty Ltd, Sydney). The glassy metal ribbons used were produced by the CSIRO Division of Applied Physics. The ribbons have a composition of $Fe_{60}Ni_{20}B_{10}Si_{10}$ and dimensions of 0·75 mm wide by 39·5 μm thick. Short ribbons of average cut length 5 mm were used as reinforcement. The formulations of the various epoxy composites studied are shown in Table 1.

The details of the preparation and testing of epoxies were similar to those described by Kinlock *et al.*[4] Three different methods were employed to disperse the ribbons uniformly in the epoxy matrix to produce four different types of ribbon–epoxy composites, namely REC, AEC1 AEC2 and CEC respectively. REC composites were fabricated by initially introducing a small quantity of short Al_2O_3 fibres into the epoxy matrix to increase its viscosity before the short ribbons were randomly added so that the tendency for premature sedimentation was minimized. AEC composites were prepared by initially casting a mixture of short ribbons and epoxy matrix into the mould. This mould was then placed between the poles of a large permanent magnet. The strong magnetic fields generated serve to align the ribbons in one direction. After curing, the sheet was machined into compact-tension specimens with ribbons aligned either parallel (AEC1) or perpendicular (AEC2) to the loading axis. A unique technique was devised to fabricate the CEC composites. Essentially, continuous ribbons were aligned parallel to each other with the aid of two perforated dies. The dies were threaded with ribbons and slotted into the mould. A standard curing schedule at 120°C for 16 h was adopted for all the fabricated composites to produce sheets of 6 mm thick.

TABLE 1
Formulation of Glassy Metal Epoxy Composites

Composite system	*Compositions (phr)*[a] *Epoxy:piperidine:rubber:alumina:glassy metal*
Rubber modified epoxy resin	100:5:15:0 :0
REC	100:5:15:3·6:0–15
AEC	100:5:15:0 :0–15
CEC	100:5:15:0 :0–15

[a] phr = parts per hundred by weight of resin.

The critical stress intensity factors, K_{Ic}, at crack initiation and subsequent crack growth were determined on samples with the compact-tension (CT) specimen geometry with an initial crack length of 20 mm. Tests were conducted in an Instron 1195 machine at ambient temperature and a crosshead speed of 1·0 mm min^{-1}. The fracture surfaces of tested materials were subsequently coated with a thin layer of platinum for examination under a JOEL 35-C scanning electron microscope.

3 RESULTS

The load, P, versus displacement, δ, curves for the various epoxy materials are shown in Fig. 1. In the epoxy systems containing short ribbons which were randomly distributed (REC) the amount of 'stick-slip' crack growth increases with the volume fraction of ribbons introduced (Fig. 1a). When the short ribbons were magnetically aligned perpendicular (AEC1) to the path of crack propagation, the cracking behaviour is very similar to that described above (Fig. 1b). However, the frequency of 'stick-slip' events decreases significantly when the short ribbons were aligned parallel to the crack path (AEC2) (Fig. 1c). There is no 'stick-slip' observed when continuous ribbons were aligned perpendicular to the crack path (CEC) Fig. 1d).

As shown in Fig. 2 the fracture properties of the epoxy matrix are significantly enhanced by the presence of ribbons. The fracture toughness measured at the maximum load of the first 'stick-slip' and the corresponding crack length at the onset of 'slip' increases with increasing ribbon content but no saturation value of K_{Ic} has yet been obtained. The largest K_{Ic} value at some crack lengths later (Fig. 3) can also be used to show that it increases with ribbon content so that this observation is generally true. Note that the crack length to calculate K_{Ic} at the maximum load of the first stick-slip (Fig. 2) is equal to the initial crack length, a_0 (20 mm), plus the stable crack growth, Δa_s, which is approximately 1–2 mm for all the composites in this CT geometry. Magnetically aligned ribbons which are perpendicular to the crack path (AEC1) appear to impart the highest fracture resistance to the epoxy matrix. The highest K_{Ic} value of 4·24 MPa$\sqrt{\text{m}}$ obtained here is in fact higher than our previously reported value of 3·85 MPa$\sqrt{\text{m}}$ (see Ref. 9) for a rubber/Al_2O_3 epoxy hybrid. K_{Ic} values for the AEC2 composites are similar to the CEC composites up to $v_f = 0{\cdot}009$; but they are larger than the toughness values of the REC composites at all volume fractions of ribbons. In order to explain these results it is important to realise that although the ribbons in AEC2 are aligned parallel to the crack path, because of the finite width (0·75 mm) and length (5 mm) of the ribbons, debonding and pull-out of

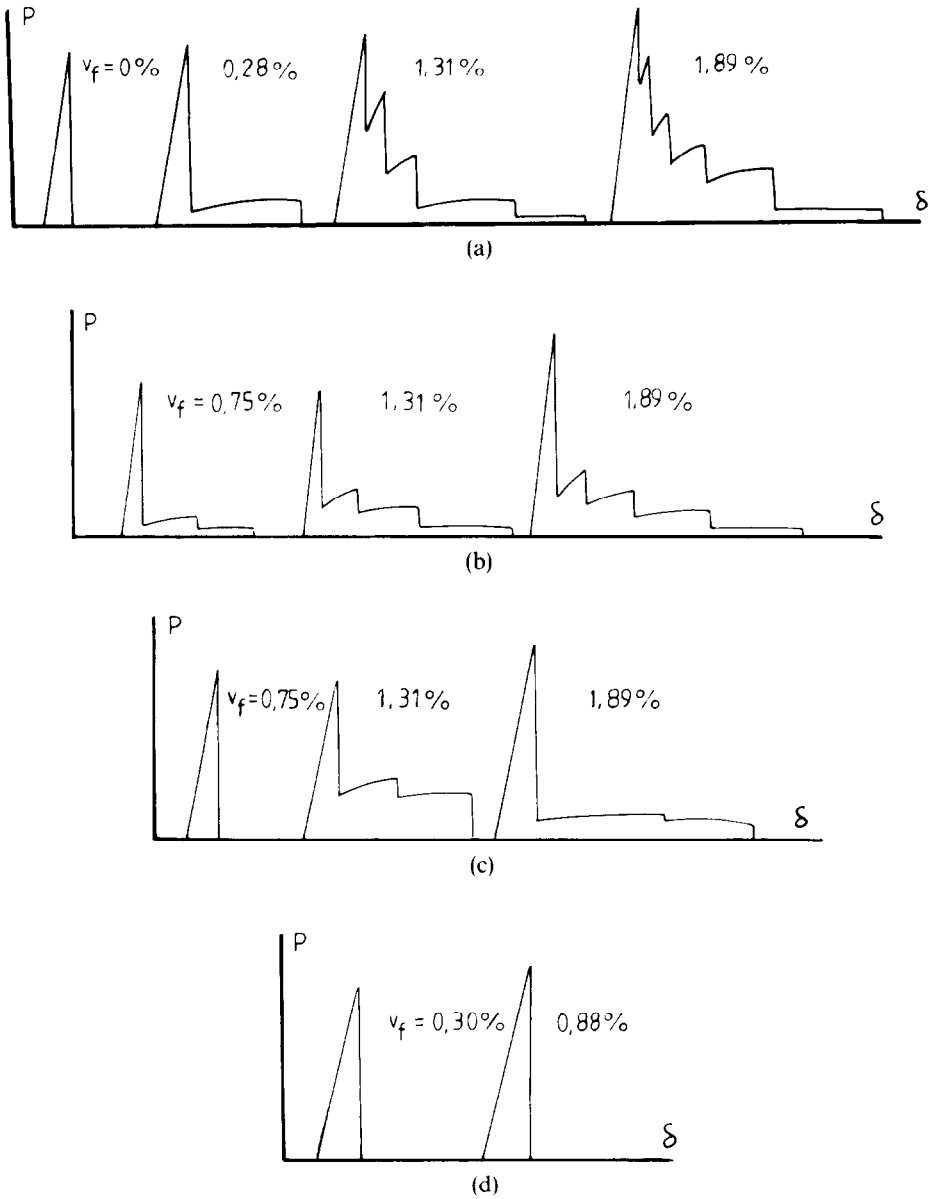

Fig. 1. Typical load–displacement (P–δ) curves for (a) REC, (b) AEC1, (c) AEC2 and (d) CEC compact tension specimens.

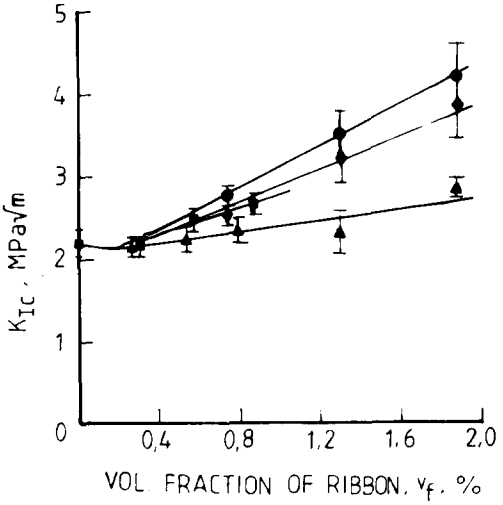

Fig. 2. Variation of K_{Ic} (calculated at maximum load of first 'stick-slip') with volume fraction of glassy metal ribbon for various composites. ● AEC1; ▲ REC; ■ CEC; ◆ AEC2.

ribbons can occur if the crack plane is perpendicular to the width direction (i.e. parallel to the normal) of these ribbons (see Fig. 7b). Of course, if the crack plane is parallel to the width direction (i.e. perpendicular to the normal) of these ribbons, since the thickness is very small (39·5 μm) there can be no debonding and pull-out mechanisms. Thus, provided the total debonded and pull-out surface areas of the ribbons are comparable to the AEC1 composites, the AEC2 composites will have similar fracture toughness as shown in Fig. 2. That the REC composite toughnesses are less

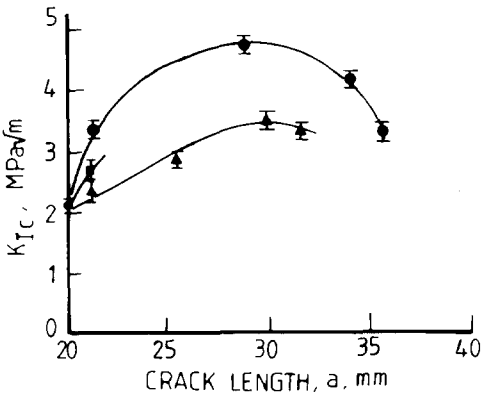

Fig. 3. Variation of K_{Ic} with crack length for (a) ● AEC1 ($v_f = 0{\cdot}0131$); (b) ▲ REC ($v_f = 0{\cdot}0131$); and (c) ■ CEC ($v_f = 0{\cdot}0088$). Note that crack initiation starts at the same matrix toughness value K_m for these ribbon reinforced composites.

than those of the AEC2 composites may be explained in terms of the random distribution of the ribbons within the matrix. The effectiveness of the ribbon debond and pull-out mechanisms is determined by an orientation efficiency factor, η, which is equal to 0·637 for 2-D randomness and 0·41 for 3-D randomness. It is not possible to compare the fracture toughness results of the CEC composites with those reported in Refs 14 and 15 because the resin matrices are different and the fracture mechanisms are unidentical (see Section 4). Our matrix material is rubber toughened with a toughness value of $2\,\text{MPa}\sqrt{\text{m}}$ whereas the pure epoxy resin matrix used by Friedrich *et al.*[14,15] has a K_{Ic} value of $0{\cdot}75\,\text{MPa}\sqrt{\text{m}}$.

In epoxy materials containing a large volume fraction of short ribbons either distributed randomly (REC) or magnetically aligned (AEC), the fracture toughness values calculated at the maximum load of each 'stick-slip' increase with crack length essentially giving rise to a K_R curve as shown in Fig. 3. Apparently, the magnetically aligned ribbons perpendicular to the crack path provide the most effective reinforcement in terms of crack toughness enhancement. The fracture mechanisms that give high K_{Ic} values with crack size are discussed in Section 4. The drop in K_{Ic} after the plateau value is due to the crack approaching the free face of the compact tension specimen thus reducing the toughening mechanisms operating behind the crack tip.

Scanning electron microscopy of fracture surfaces shows that in the absence of any glassy metal ribbons, the river markings formed tend to radiate outwards from the crack initiation focal region. These river markings consist of discontinuous cleavage steps which follow the direction of crack growth (Fig. 4). The overall fracture surface features are not significantly altered for the randomly distributed ribbon composites (REC) with a small amount of ribbons (Fig. 5a) except at the localized region in the vicinity of the ribbon where an enhanced plastic flow of the matrix may be observed (Fig. 5b). Shear steps may also be seen to emanate at inclined angles from the interface. Most of the ribbons are pulled-out rather than fractured. However, some ribbons appear to remain strongly bonded at the interface (Fig. 5b) while others have clearly been debonded (Fig. 5c). Clean pull-out is observed for the already debonded ribbons while a substantial plastic bending and shearing occurs during pull-out of the strongly bonded ribbons inclined at an oblique angle to the crack plane (Fig. 6a). The extent of the shear-induced steps becomes greater with increasing ribbon content and so is the frequency of ribbon pull-out. A much rougher fracture surface with extensive plastic-shear deformation is also observed at high volume fractions of ribbon (Fig. 6b). Similar microstructural features are displayed in the epoxy composites containing magnetically aligned short ribbons (AEC) (Fig. 7) although the effects are more pronounced. Contrasting

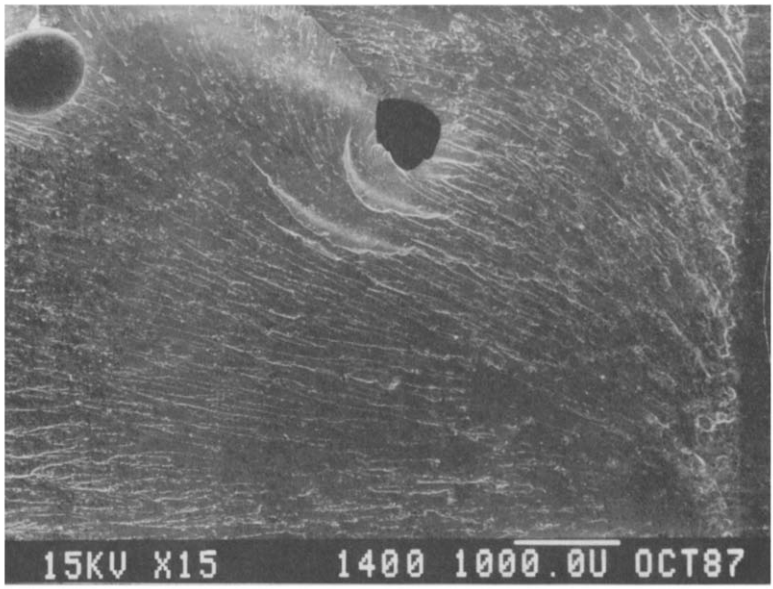

Fig. 4. Fracture surface of epoxy containing no ribbon, showing typical river-like patterns.

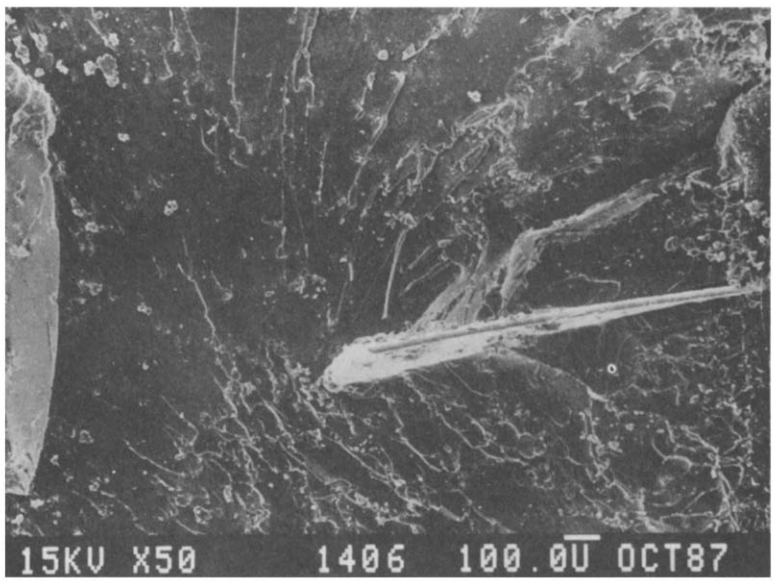

(a)

Fig. 5. Fracture surfaces of REC epoxy composite containing 2 phr ribbon showing (a) a pulled-out ribbon standing proud near the site of crack initiation at extreme right; (b) a pulled-out ribbon with severe deformation of the matrix material; and (c) a debonded ribbon with no matrix plastic deformation.

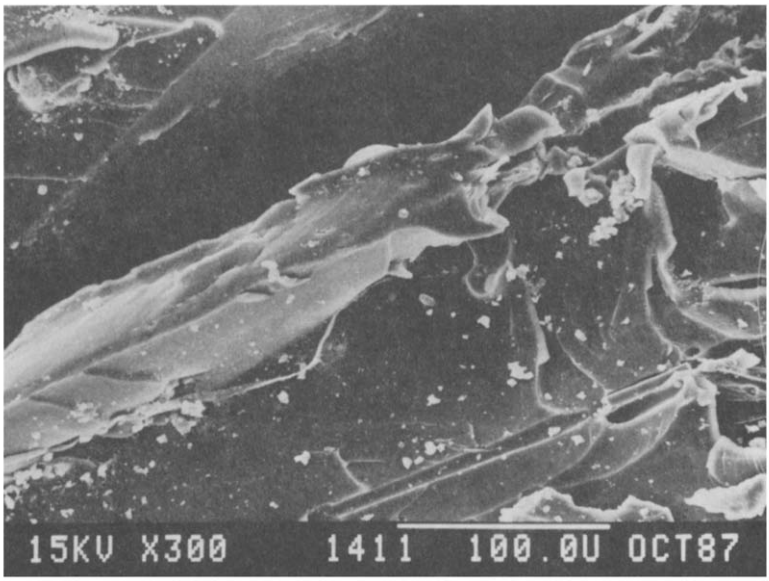

(b)

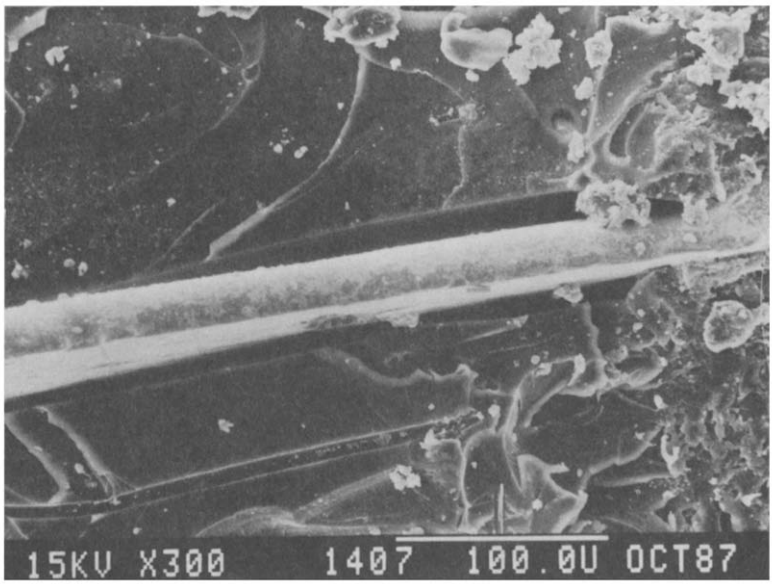

(c)

Fig. 5—*contd.*

(a)

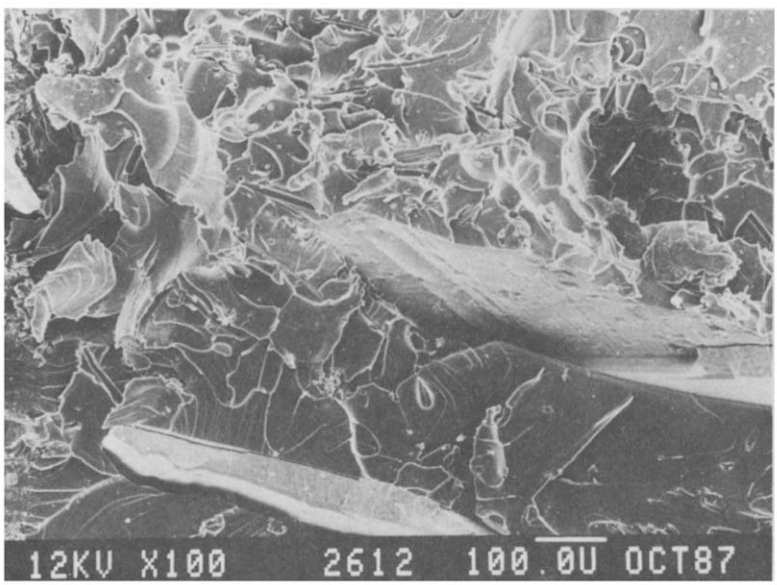

(b)

Fig. 6. Fracture surfaces of REC composites containing 15 phr ribbon showing (a) crack initiation at left and there is clear evidence of ribbon debonding, pull-out and plastic bending and shear of ribbons; and (b) fractured ribbons and extensive deformation of matrix material.

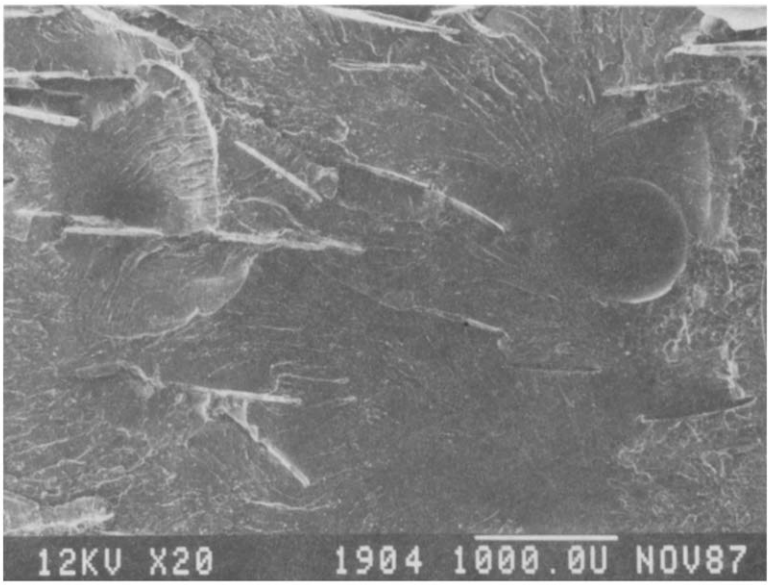

(a)

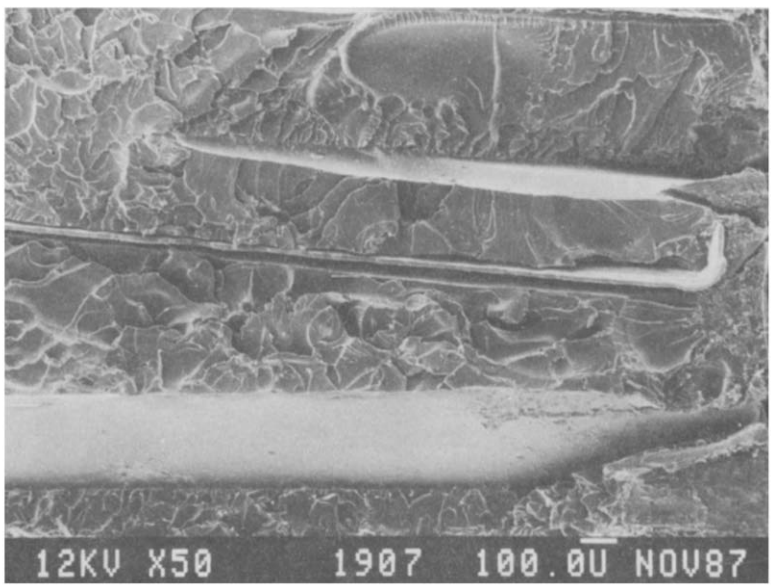

(b)

Fig. 7. Fracture surfaces of AEC composites containing 15 phr ribbon showing (a) oriented ribbons perpendicular to crack plane are either fractured or debonded prior to being pulled-out (AEC1); and (b) fracture along lengthwise direction of ribbon showing ribbon debond and pull-out (AEC2).

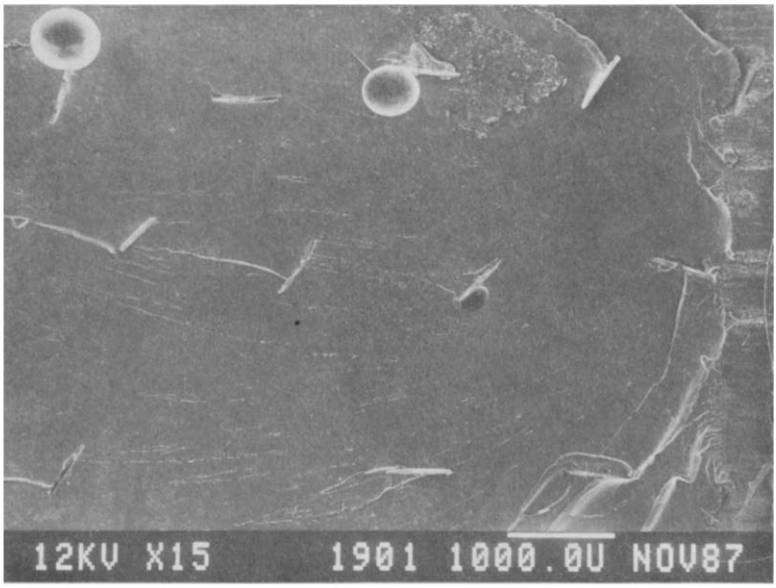

(a)

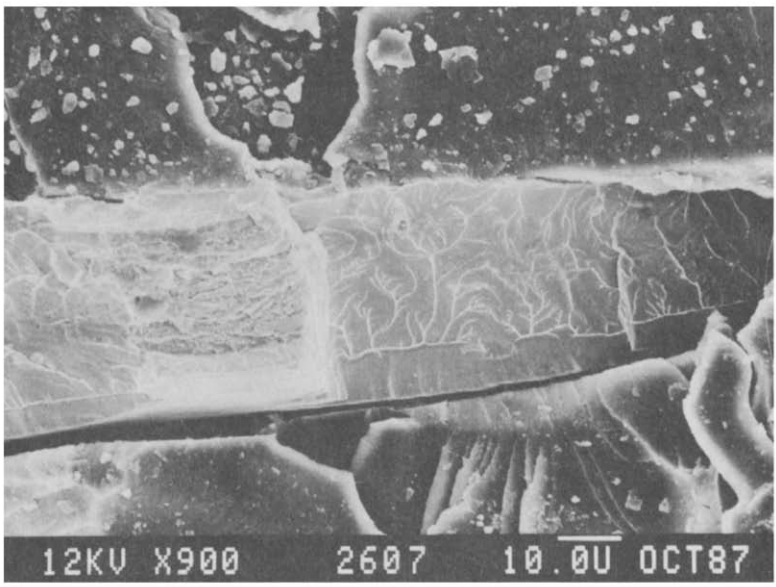

(b)

Fig. 8. Fracture surfaces of CEC composites containing 0·88% ribbon by volume. (a) Relatively smooth fracture surface showing crack pinning by the ribbons. (b) The fractured ribbon lying on the same plane as the crack shows no pull-out and no debonding.

microstructural features are observed in the composites containing continuous ribbons (CEC) (Fig. 8a) which display much similarity with the fracture surface of Fig. 4 where fine river markings and smooth cleavage steps are formed. The presence of these ribbons does not appear to cause much plastic-shear flow nor are they pulled-out. All the ribbons appear to fracture (Fig. 8b) with little noticeable debonding at the interface and they tend to pin the crack fronts in producing the typical 'tail' steps.

4 DISCUSSION

A perusal of the cracking behaviour in the ribbon modified epoxies (Fig. 1) and their associated fracture toughness values (Figs 2 and 3) suggest that glassy ribbons, especially short ones, can impart a considerable improvement in the fracture resistance to the epoxy matrix. These composites also produce a crack propagation mode with multiple 'stick-slips'. The origins of this crack jumping phenomenon have been attributed to various mechanisms that have previously been discussed in some detail.[18] Briefly, this can be due to a positive dG/da,[19] a negative dK_{Ic}/da (Ref. 20) or $dK_{Ic}/d\dot{a}$ (Ref. 21) and crack tip blunting.[22] Here G is the potential energy release rate and $\dot{a}$ is the crack velocity.

The results of the present study (Fig. 1) clearly indicate that the frequency of crack jumping tends to increase with the volume fraction of short ribbons that lie in the crack plane. This also suggests that there is a strong correlation between the frequency of 'stick-slips' and the extent of crack tip–ribbon interactions. We believe that the 'stick' process arises from a series of sequential events due to crack tip tilting and twisting (i.e. crack deflection), crack tip blunting, crack bridging and ribbon pull-out. The crack extends stably in the 'stick' process as can be seen from the non-linear portion of the load–displacement curve prior to the maximum load shown in Fig. 1. The 'slip' process corresponds to the precipitous load drop because the strain energy release from the blunted crack tip is more than required to propagate the crack. The unstable crack will run for a considerable distance until all the excess energy is used up and the crack will be arrested. The distance at which the crack may be arrested depends on the extent of energy dissipation ahead and more importantly at the wake of the crack tip. The presence of numerous short ribbons in the plane of crack propagation would invariably lead to a large energy dissipation associated with crack deflection, interface debonding, ribbon pull-out and crack bridging. Consequently, the crack is arrested much faster and the load drop is less. This would allow repetitions of the crack jumping process to occur and give rise to the observed multiple 'stick-slip' cracking behaviour (Fig. 1a and b). It follows therefore that in the

absence of ribbons, the excess energy may not be sufficiently used up to produce crack arrest and brittle fracture with no 'stick-slip' is obtained (Fig. 1a). Similar cracking behaviour may be obtained if the presence of ribbons is not able to consume the excess strain energy owing to inadequate work dissipating processes (Fig. 1d).

Qualitatively, the multiple 'stick-slip' and variation of K_{Ic} with crack length can be interpreted in terms of the crack resistance curve concept. The crack resistance curve (K_R–Δa) is shown in Fig. 9 and the applied stress intensity factor, K_a, curves for constant stress and different crack lengths are also superposed. Assuming that the initial crack length of the compact tension specimen is a_2, i.e. curve 2 for K_a, stable crack growth (or stick) occurs under increasing applied stress until this curve is tangential to the K_R curve at point F at which fracture instability (or slip) occurs. In tests in load-controlled machines the crack will not be arrested but in displacement-controlled machines (such as the Instron 1195) the crack may be arrested. The new crack length is now equal to a_2 plus Δa_s and the amount of fast crack growth prior to arrest. Assume this to be a_3 and that the stable crack growth–fracture instability (and arrest) event will repeat itself. This time the point of tangency is moved up to G. The instability K_{Ic} therefore increases with crack length as shown in Fig. 3. The amount of stable crack growth which is due to the various toughening mechanisms already described also increases with crack length. As explained previously the drop in K_{Ic} at large

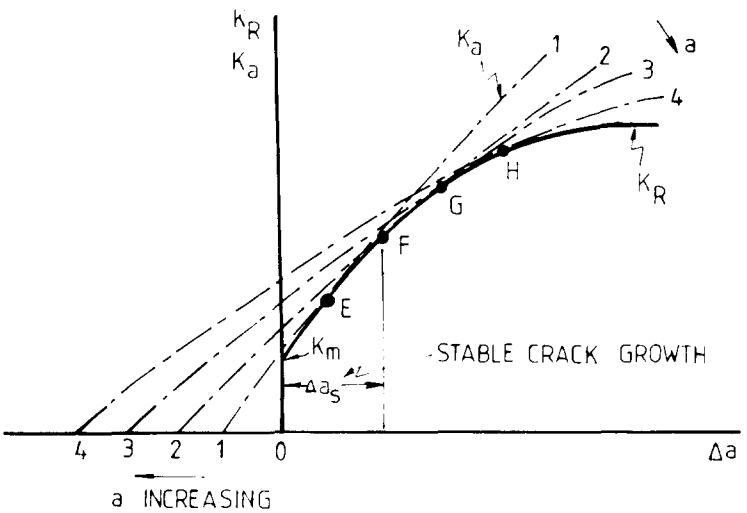

Fig. 9. Schematic using the crack resistance curve concept to explain the increasing K_{Ic} with crack length a and the multiple 'stick-slip'. The K_R curve starts at the resin matrix toughness value K_m at $\Delta a = 0$.

crack lengths (Fig. 3) is because the crack is near the free face of the specimen and is affected by it. (The finite size of the ligament of the compact tension specimen is about 40 mm and there is an initial crack size of some 20 mm).

The micromechanisms of fracture are clearly different in short and continuous ribbon reinforced epoxies. These differences may be readily elucidated from the understanding of the distribution of stresses along the length of the ribbon. At the ends of the ribbon there is zero tensile stress, σ, but it builds up to the ribbon tensile strength, σ_f, at half the critical length, l_c. On the other hand, large shear stresses, τ, are developed at the ribbon ends which gradually drop to zero at the position $l_c/2$ along the length direction. Now in epoxies containing short ribbons, numerous ribbon ends provide sites for development of large shear stresses which may induce interface debonding when the shear strength is reached before the ribbon reaches its tensile strength. Thus, with increasing load, the ribbon ends are gradually debonded at an increasing extent. As the advancing crack tip meets the debonded ribbons, it initially tilts along the interface but ultimately undergoes twisting between ribbons.[23] Some of the debonded ribbons will also bridge the fracture plane behind the crack tip. They will be pulled-out gradually as the crack opening displacement increases. Some of these ribbons will fracture and then pull-out. These fracture processes invariably lead to a non-planar fracture surface as a result of the crack front moving locally in different directions at different positions across the specimen thickness. In addition there is clear evidence of the formation of extensive shear steps around and between ribbons. Thus, the concurrent display of crack bridging by the ribbons, rubber particles and unbroken matrix ligaments through the thickness of the specimens act in concert to produce a rising crack resistance curve. The more prominent K_R curve observed in the AEC1 composites can be attributed to a higher volume fraction of ribbons that lie in the plane of crack growth (Fig. 3).

For the epoxies containing continuous ribbons, absence of ribbon ends in the crack plane neighbourhood means that no easy debonding can occur and the ribbons fracture at the crack plane (Fig. 8b) so that no ribbon pull-out is observed. In a way this implies that there is sufficiently good bonding between ribbon and epoxy resin to ensure that the ribbon strength is utilised. The crack therefore propagates relatively unimpeded through the composite. The fracture resistance arises mainly from the work done in deforming and breaking the ribbons and the epoxy resin matrix in the path of the planar crack. The presence of the ribbon may, nonetheless, also pin the crack front and impart some fracture resistance to the composite (Fig. 8a). However, the toughening mechanisms for these continuous ribbon composites are considerably less compared with the short ribbon composites. Therefore, there is only an insignificant K_R curve observed for

the CEC composites as given in Fig. 3. In the CEC composites studied by Friedrich *et al.*[14,15] the failure mechanisms are quite different to those reported above for our CEC composites. Instead these mechanisms are rather similar to our REC and AEC composites i.e. ribbon debond, fracture and pull-out, matrix deformation, as well as plastic bending of ribbons etc. We cannot offer any satisfactory explanation for the different failure behaviours of these two types of CEC composites.

5 CONCLUSIONS

Epoxy composites containing short and continuous amorphous metal ribbons have been fabricated and evaluated. Considerable improvements in the fracture toughness, K_{Ic}, were recorded.

The results suggest that K_{Ic} values of greater than $4\,MPa\sqrt{m}$ may be obtained for ribbon content, v_f, higher than 0·019. The sources of toughening mechanisms are identified and discussed in relation to the microstructures. These include: crack deflection, interface debonding, crack bridging, plastic deformation and bending of ribbons as well as enhanced plastic-shear yielding or flow in the vicinity of the crack tip.

Failure of these epoxy composites was particularly sensitive to the interfacial properties. A high toughness and large degree of flaw tolerance may be achieved when a large extent of debonding occurs along the interface (e.g. the AEC composites). On the other hand, absence of debonding at the interface tends to give a weak and brittle composite material (e.g. the CEC composites).

ACKNOWLEDGEMENTS

We wish to thank the CSIRO (Division of Applied Physics) for providing the glassy metal ribbons and allowing us to make use of their large permanent magnets to align the ribbons. We also thank the Electron Microscopic Unit of Sydney University for putting its facilities at our disposal. Financial support by the Sydney County Council and the Department of Defence (Materials Research Laboratories) is much appreciated.

REFERENCES

1. Moloney, A. C., Kausch, H. H. & Stieger, H. R., *J. Mater. Sci.*, **18** (1983) 208.
2. Spanoudakis, J. & Young, R. J., *J. Mater. Sci.*, **19** (1984) 473.

3. Low, I. M. & Mai, Y.-W., *Proc. Int. Conf. on Future trends in plastics and rubber technology*, Singapore, September 1987.
4. Kinloch, A. J., Shaw, S. J., Tod, D. A. & Hunston, D. L., *Polymer*, **24** (1983) 1341.
5. Kunz-Douglass, S., Beaumont, P. W. R. & Ashby, M. F., *J. Mat. Sci.*, **15** (1980) 1109.
6. Bascom, W. D., Ting, R. Y., Moulton, R. J., Riew, C. K. & Siebert, A. R., *J. Mater. Sci.*, **16** (1981) 2657.
7. Maxwell, D., Young, R. J. & Kinloch, A. J., *J. Mater. Sci. Lett.*, **3** (1984) 9.
8. Kinloch, A. J., Maxwell, D. & Young, R. J., *J. Mater. Sci.*, **20** (1985) 4169.
9. Low, I. M., Mai, Y.-W., Bandyopadhay, S. & Silva, V. M., *Materials Forum*, **10** (1987) 241.
10. Argon, A. S., Hawkins, G. W. & Kuo, H. Y., *J. Mater. Sci.*, **14** (1979) 1707.
11. Chand, N., Das, S. & Rohatgi, P. K., *J. Mater. Sci. Lett.*, **5** (1986) 823.
12. Yeow, Y. T., *Composites*, **17** (1981) 139.
13. Yeow, Y. T., *J. Mater. Sci.*, **17** (1982) 2245.
14. Fels, A., Friedrich, K. & Hornbogen, E., *J. Mater. Sci. Lett.*, **3** (1984) 569.
15. Friedrich, K., Fels, A. & Hornbogen, E., *Comp. Sci. & Techn.*, **23** (1985) 79.
16. Gilman, J. J., *Metal Progress*, **116** (1979) 1.
17. Strife, J. R. & Prewo, K. M., *J. Mater. Sci.*, **17** (1982) 359.
18. Garg, A. C. & Mai, Y. W., *Comp. Sci. & Techn.*, **18** (1988) 179.
19. Gurney, C. & Mai, Y.-W., *Eng. Fract. Mech.*, **4** (1972) 853.
20. Mai, Y.-W., *Int. J. Fract.* **10** (1974) 292.
21. Mai, Y.-W. & Atkins, A. G., *J. Mater Sci.*, **10** (1975) 2000.
22. Kinloch, A. J. & Williams, J. G., *J. Mater. Sci.*, **15** (1980) 987.
23. Faber, K. T. & Evans, A. G., *Acta Metall.*, **31** (1983) 565.